LASERS

PACS numbers: 42.55.Px; 42.25.Ja
DOI: 10.1070/QE2011v041n10ABEH014699

Measuring the Stokes parameters of radiation of semiconductor lasers

N.V. D'yachkov, A.P. Bogatov

Abstract. **We have developed and tested an original method for measuring the Stokes parameters for semiconductor lasers, based on the binding of the coordinate system to the test sample. The proposed method, when using an arbitrary phase plate as a compensator, allows one to measure the polarisation characteristics of lasers operating in a wide range of wavelengths – from 600 to 1000 nm. Application of the Fourier analysis to the quasi-continuous experimental data obtained with the help of automated systems of acquisition and processing of measurement results and ordinary optical elements provides accuracy that is sufficient to record the peculiarities of the polarisation characteristics of modern laser diodes.**

Keywords: *semiconductor lasers, heterolaser, radiation polarisation, Stokes parameters.*

1. Introduction

Stokes parameters are the main characteristics of any radiation because they can more fully describe the state and degree of polarisation. In the case of a diode heterolaser, Stokes parameters, apart from the characteristic of the polarisation properties of radiation, also contain information about the internal optical inhomogeneities of the cavity [1], which can be useful for diagnosing the quality of the laser itself. With some degree of conditionality, we can assume that the process of measuring the Stokes parameters for a diode laser is similar to the study of its cavity in crossed polarisers. In this case, optical probing is performed by intracavity radiation of the laser itself, which propagates in the spatial cavity regions that greatly affect the characteristics of the laser diode. In particular, the level of optical inhomogeneities can serve as a quantitative characteristic of technological imperfections of a specific sample or a batch of samples prepared by the same technology. From this point of view, the Stokes parameters are of particular interest for diode lasers.

The classical method for measuring the Stokes parameters [2] is not optimal with respect to the diode laser in the light of possible automation of these measurements with the help of personal computers and data acquisition systems. For example, it involves the use of a quarter-wave plate, which, due to the dispersion, has a limited spectral range, whereas the working wavelength of widely used diode lasers vary in a wide spectral range – from 0.4 to 1.6 μm.

In this paper, we propose the simplest (from our point of view) technique for measuring the Stokes parameters, which implies the use of an arbitrary phase plate and allows the measurements to be performed in a wide range of wavelengths on the same setup. By automating the measurements, collecting and processing large amounts of data in a single process, this method ensures measurement accuracy acceptable for a semiconductor laser using a relatively simple setup.

N.V. D'yachkov, A.P. Bogatov P.N. Lebedev Physics Institute, Russian Academy of Sciences, Leninsky prosp. 53, 119991 Moscow, Russia; e-mail: kln40@yandex.ru

Received 22 July 2011
Kvantovaya Elektronika **41** (10) 869–874 (2011)
Translated by I.A. Ulitkin

2. Optical scheme and measurement technique

The optical scheme of the setup measuring the Stokes parameters is shown in Fig. 1. Diode laser radiation, focused into a parallel beam, passes through a phase plate and a polariser (analyser) and enters the photodetector. The coordinate system XYZ is chosen so that the direction of the Z axis coincide with the radiation propagation direction and the X axis be parallel to the plane of the structure layers of the laser diode under study.

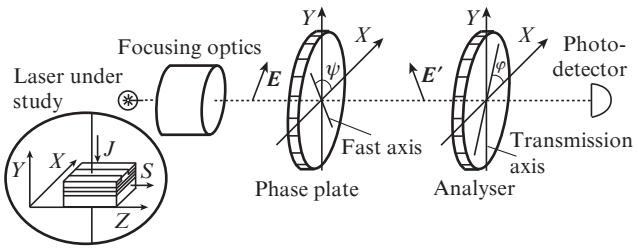

Figure 1. Optical scheme of the setup for measuring the Stokes parameters: S is the normal to the output facet of the laser diode; J is the direction of the laser pump current.

The change in the polarisation state of monochromatic light passing through such an optical system is described most simply by means of Jones matrices [3]. In the case of quasi-monochromatic radiation, use can made of a similar description, assuming that the Jones vector $\boldsymbol{V}$ of radiation changes slowly with time, which corresponds to the following time dependence of the complex electric field vector:

$$\bar{\boldsymbol{E}}(t) = \begin{pmatrix} E_x(t) \\ E_y(t) \end{pmatrix} = \begin{pmatrix} V_x(t) \\ V_y(t) \end{pmatrix} \exp(-\mathrm{i}\omega t) \ . \qquad (1)$$

Here, ω is the central frequency of the optical radiation spectrum, and the complex functions $V_x(t)$ and $V_y(t)$ are the reali-

sations of stationary random processes. The polarisation state of this radiation is completely determined by the Stokes parameters, which are expressed through the time-averaged products of the components of the specified vectors [2]:

$$\begin{aligned} s_0 &= \langle E_x E_x^* \rangle + \langle E_y E_y^* \rangle \equiv \langle V_x V_x^* \rangle + \langle V_y V_y^* \rangle; \\ s_1 &= \langle E_x E_x^* \rangle - \langle E_y E_y^* \rangle \equiv \langle V_x V_x^* \rangle - \langle V_y V_y^* \rangle; \\ s_2 &= \langle E_x E_y^* \rangle + \langle E_y E_x^* \rangle \equiv \langle V_x V_y^* \rangle + \langle V_y V_x^* \rangle; \\ s_3 &= \mathrm{i}(\langle E_y E_x^* \rangle - \langle E_x E_y^* \rangle) \equiv \mathrm{i}(\langle V_y V_x^* \rangle - \langle V_x V_y^* \rangle). \end{aligned} \tag{2}$$

Note that the averaged products in (2) are the elements of the coherence matrix, each of which can be uniquely expressed by a linear combination of the Stokes parameters. The Stokes parameters, in turn, have a clear physical interpretation according to which the zero parameter (s_0) is equal to the average total intensity of the beam, while the remaining three parameters represent the difference between the intensities of the components of the beam expansion in various bases. In this case, for the first (s_1) and second (s_2) parameters use is made of linearly polarised basic states, where the vector $\boldsymbol{E}$ is inclined to the X axis at various angles, and for the third (s_3) state use is made of basic states with the right (R) and left (L) circular polarisation:

$$\begin{aligned} &s_0 = I(0) + I(\pi/2), \quad s_1 = I(0) - I(\pi/2), \\ &s_2 = I(\pi/4) - I(3\pi/4), \quad s_3 = I_\mathrm{R} - I_\mathrm{L}. \end{aligned} \tag{3}$$

In our coordinate system, taking into account the binding to the plane of the laser structure layers, the quantities $I(0)$ and $I(\pi/2)$ are the intensity of the TE and TM components of laser radiation.

In this paper, as the parameters describing polarisation, we used three reduced (normalised to the total intensity of the beam) Stokes parameters:

$$S_1 = s_1/s_0; \quad S_2 = s_2/s_0; \quad S_3 = s_3/s_0. \tag{4}$$

It is easy to show that the intensity I of radiation passing through the above-described optical system can be uniquely expressed in terms of the Stokes parameters s_i of radiation under study, rotation angles of the transmission axis φ of the analyser and the fast axis ψ of the phase plate with respect to the X axis, as well as in terms of the phase difference α (introduced by the plate) between the components of radiation polarised along its fast and slow axes. If we choose a new coordinate system $X'Y'Z$ so that the axis X' coincide with the transmission axis of the analyser (the angle between the axes X' and X is equal to φ), the intensity of radiation passing through the analyser will be equal to $\langle |E'_{x'}|^2 \rangle$ – the averaged square of the component $\boldsymbol{E}'(t)$ of the vector, and the coordinates of the vector $\boldsymbol{E}'(t)$ in the coordinate system $X'Y'$ will be bound to the coordinates of the vector $\boldsymbol{E}(t)$ in the XY system by the product of the rotation matrix and the Jones matrix for phase plate (similarly to the binding of the Jones vectors, given in [3]):

$$\begin{aligned} &\begin{pmatrix} E'_{x'}(t) \\ E'_{y'}(t) \end{pmatrix} = R(\varphi - \psi) W_\alpha R(\psi) \begin{pmatrix} E_x(t) \\ E_y(t) \end{pmatrix}, \\ &R(\theta) = \begin{pmatrix} \cos\theta & \sin\theta \\ -\sin\theta & \cos\theta \end{pmatrix}, \quad W_\alpha = \begin{pmatrix} \exp(-\mathrm{i}\alpha/2) & 0 \\ 0 & \exp(\mathrm{i}\alpha/2) \end{pmatrix}. \end{aligned} \tag{5}$$

Expressions (5) implies that the desired intensity $I = \langle |E'_{x'}|^2 \rangle$ is a linear combination of the elements of coherence matrix, and, therefore, the Stokes parameters. Using simple trigonometric transformations, we can reduce the expression for this quantity to the form [4]:

$$\begin{aligned} I(\varphi,\psi,\alpha) &= \frac{s_0}{2} + \frac{1}{2} s_3 \sin[2(\varphi - \psi)] \sin\alpha + \frac{1}{4}(s_1 \cos 2\varphi \\ &+ s_2 \sin 2\varphi)(1 + \cos\alpha) + \frac{1}{4}[(s_1 \cos 2\varphi - s_2 \sin 2\varphi)\cos 4\psi \\ &+ (s_1 \sin 2\varphi + s_2 \cos 2\varphi)\sin 4\psi](1 - \cos\alpha). \end{aligned} \tag{6}$$

We assume below that the phase plate is turned so that the fast axis is first directed along the X axis ($\psi = 0$), and then – along the Y axis ($\psi = \pi/2$). In this case, the expression for the radiation intensities, normalised to their average values over the period, takes the form

$$\begin{aligned} I_0(\varphi,\alpha) &= \frac{\pi k I(\varphi,0,\alpha)}{\int_0^{\pi k} I(\varphi,0,\alpha)\mathrm{d}\varphi} = 1 + S_1 \cos 2\varphi \\ &+ (S_2 \cos\alpha + S_3 \sin\alpha)\sin 2\varphi, \\ I_{\pi/2}(\varphi,\alpha) &= \frac{\pi k I(\varphi,\pi/2,\alpha)}{\int_0^{\pi k} I(\varphi,\pi/2,\alpha)\mathrm{d}\varphi} = 1 + S_1 \cos 2\varphi \\ &+ (S_2 \cos\alpha - S_3 \sin\alpha)\sin 2\varphi, \end{aligned} \tag{7}$$

where k is a natural number. We express the reduced Stokes parameters through the Fourier components of these functions

$$\begin{aligned} a(\psi) &= \frac{2}{\pi k} \int_0^{\pi k} I(\varphi,\psi,\alpha)\cos 2\varphi \mathrm{d}\varphi, \\ b(\psi) &= \frac{2}{\pi k} \int_0^{\pi k} I(\varphi,\psi,\alpha)\sin 2\varphi \mathrm{d}\varphi \end{aligned} \tag{8}$$

in the form:

$$\begin{aligned} &S_1 = a(0) = a(\pi/2), \quad S_2 = \frac{b(0) + b(\pi/2)}{2\cos\alpha}, \\ &S_3 = \frac{b(0) - b(\pi/2)}{2\sin\alpha}. \end{aligned}$$

This means that to determine the Stokes parameters of the radiation under study with the help of the system described above, it is sufficient to measure the dependence of the signal from the photodetector on the angle of rotation of the analyser at two different (corresponding to $\psi = 0$ and $\psi = \pi/2$) positions of the phase plates, for which trigonometric functions of the parameter α are known. Because the values of the trigonometric functions do not contain information about the sign of the argument, we use for definiteness the axis with $\sin\alpha > 0$ as the fast axis.

Thus, if the Fourier components $a(\psi)$ and $b(\psi)$, as well as the values of $\cos\alpha$ and $\sin\alpha$ are known for the phase plate, we can determine all the Stokes parameters. Expressions (8) and (9) were used in our method to find the Stokes parameters. Note that to determine $\cos\alpha$ and $\sin\alpha$, it is necessary to precalibrate the phase plate.

3. Experimental setup and calibration of the plate

As the phase plate, we used an arbitrarily cleaved mica plate with the thickness of several tens of micrometres. The plate was placed between two glass substrates having the thickness of ~2 mm each, the space between them being filled with immersion oil. This design of the phase plate, in addition to protection against mechanical strains, provides suppression of possible spurious interference effects in a thin plate.

The scheme of the setup for the phase plate calibration is shown in Fig. 2. It includes, apart from the tested laser and calibrated plate, an auxiliary polariser (hereafter, a polariser), analyser, Fresnel rhomb, and photodetector. As the polariser and analyser, we used thin-film polarisers, and as the photodetector – FD-24K photodiode, embedded into the transimpedance circuit with a bias of 8 V. The signal from the photodetector was fed to the ADC input with the software-driven preamplification whose gain during the measurements was automatically adapted to the input level. This allowed us to ensure the independence of the relative accuracy of the signal measurement from its level. The phase plate and analyser were fixed in software-controlled translation stages, driven by stepper motors. In our measurements, the period T (the time of rotation of the analyser by an angle 2π) was ~30 s, and the number of measurements per revolution was equal to 1001. Therefore, the time interval between two successive measurements was $\Delta t = T/1000$.

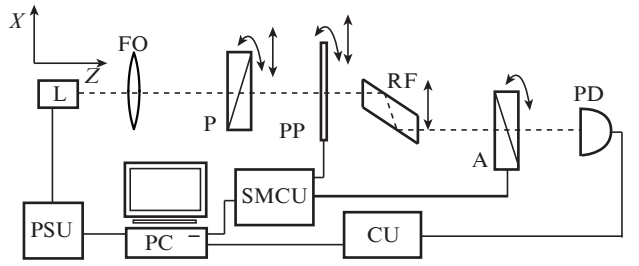

Figure 2. Scheme of the experimental setup for measuring the Stokes parameters and calibrating the used phase plate: (L) laser under investigation, placed in the holder; (PSU) digitally controlled power supply unit of the laser; (FO) focusing optics; (P) polariser; (PP) phase plate; (FR) Fresnel rhomb; (A) analyser; (PD) photodiode; (CU) control unit of the photodiode; (SMCU) stepper motor control unit; (PC) computer with a built-in DAC–ADC unit.

In the above optical scheme, the laser and polariser were actually used as a source of polarised radiation. In calibrating the plate, we first bound the initial position of the polariser and analyser to the X and Y axes, respectively. At the same time, as the X and Y axes we used the major and minor axes of the ellipse of laser radiation polarisation in the spontaneous regime, because these axes correspond most to the directions of TE and TM polarisations. Indeed, the polarisation state of the amplified spontaneous emission, primarily due to its significantly lower temporal coherence, is affected by defects in the waveguide considerably weaker than the polarisation of laser radiation and, therefore, corresponds most to the state, which is determined by the symmetry of the active region.

To set the initial position of the polarisers on these axes, we initially injected the current corresponding to the spontaneous regime of laser operation, and in the optical system consisting of the polarisation elements we had only an analyser mounted in the position corresponding to the minimum signal from the photodetector. Then, at a current corresponding to the laser regime, we introduced the polariser into the system and placed it in the position, crossed with respect to the analyser. In this case, the signal minimum from the photodetector served as the reference point. The polarisers were bound to the axes similarly and later at the stage of installation directly before the measurements of the Stokes parameters.

After establishing the initial position of the polariser, we measured $\cos\alpha$ of the plate. We introduced the plate into the system, one of the plate's axes being oriented along the X axis. The criterion for precise positioning was one of the local minima in the dependence of the signal from the photodetector on the rotation angle of the plate. In this position, one of the axes of the plate proved to be parallel to the X axis. After this, the analyser was turned by $\pi/2$ and the polariser – by $\pi/4$. In this case, the analyser should be oriented along the X axis, and the Stokes parameters of radiation at the entrance to the plate –

$$S_1 = S_3 = 0, \quad S_2 = 1. \tag{10}$$

Then, we performed a quasi-continuous measurement of the dependence $I(\varphi)$ of the signal from the photodetector on the rotation angle of the analyser in the range $0 \leqslant \varphi \leqslant 2\pi$.. The cosine of the phase shift introduced by the plate was found, according to (7) and (9), from the expression

$$\cos\alpha = \frac{2\int_0^{2\pi} I(\varphi)\sin 2\varphi \,\mathrm{d}\varphi}{\int_0^{2\pi} I(\varphi)\,\mathrm{d}\varphi}. \tag{11}$$

To find the position of the fast axis of the plate (i.e., the one for which $\sin\alpha > 0$), it is necessary to find at least the sign of the sine of the phase shift α_0, introduced by the plate, between the radiation components polarised along the X and Y axes at the current position of the plate. Note that in this case $\cos\alpha_0 = \cos\alpha$. To find $\sin\alpha_0$, we used the Fresnel rhomb. The latter can be considered as an analogue of the phase plate with the previously known positions of the fast and slow axes, which are known to be determined by the rhomb geometry. In our case, the rhomb was oriented so that its reflecting faces be parallel to the Y axis, which corresponded to the orientation of its fast axis along the X axis. In this position the rhomb makes such a phase shift β between the waves with the vector $\boldsymbol{E}$ directed along the Y or X axis that $\sin\beta > 0$. Ideally, the rhomb should provide a phase shift $\beta = \pi/2$. In a real situation β differs from $\pi/2$ for several reasons; therefore, we first should measure the $\cos\beta$ for the Fresnel rhomb. To do this, the plate was replaced by the Fresnel rhomb and the operation, described above for the phase plate, was performed.

After $\cos\beta$ was found, the phase plate was again mounted into the system. Now the optical system included the phase

plate and Fresnel rhomb, which gave the total phase shift $\gamma = \alpha_0 + \beta$. Then, we used the above described operation to find $\cos\gamma$. Knowing $\cos\alpha_0 = \cos\alpha$, $\cos\beta$ and $\cos\gamma$, it is easy to calculate $\sin\alpha_0$:

$$\sin\alpha_0 = \frac{\cos\alpha\cos\beta - \cos\gamma}{\sqrt{1-\cos^2\beta}}. \qquad (12)$$

The sign of the obtained quantity determined the actual position of the fast axis of the plate: if it is positive, the fast axis of the plate is the one that is parallel to the X axis; otherwise, it is the axis parallel to Y.

To estimate the measurement error, α, we found the cosines γ of the phase shifts, introduced by different systems composed of a Fresnel rhomb and a plate rotated relative to the initial position by angles that are multiple of $\pi/2$. The results of these measurements using a laser with a working wavelength of 665 nm are presented in Table 1. The data of this table suggest that the real value of α should be $45.3 \pm 0.6°$. Such an error, according to (9), should provide a relative accuracy of 1% in determining the second and third Stokes parameters. Table 1 also shows that the measured phase shift, introduced by the Fresnel rhomb, significantly (approximately by 20%) differs from the theoretical value of $\pi/2$.

Table 1. Results of measurements of the phase shift γ introduced by the optical elements at different orientations of the plate.

Optical system	Phase shift	$\cos\gamma$	γ/deg	α/deg
Plate in the initial position	α	0.695	45.97	45.97
Plate rotated by 180°	α	0.694	46.05	46.05
Rhomb	β	0.257	75,11	–
Rhomb+plate in the initial position	$\beta+\alpha$	−0.505	120.33	45.22
Rhomb+plate rotated by 90°	$\beta-\alpha$	0.865	30.11	45.11
Rhomb+plate rotated by 180°	$\beta+\alpha$	−0.498	119.86	44.75
Rhomb+plate rotated by 270°	$\beta-\alpha$	0.862	30.46	44.70

In this paper, we measured the parameters of laser radiation with wavelengths of 665, 850 and 980 nm. The plate was calibrated for each wavelength. The results of these calibrations are shown in Fig. 3. The figure also shows the approximating curve of type $\alpha(\lambda) = A + B/\lambda$, which corresponds to a birefringent element with the linear-wavelength dispersion of the difference between the refractive indices. The resulting graph suggests that the plate can be used to study radiation with wavelengths from 400 to 1300 nm. In this case, as follows from Fig. 3, within the arbitrary spectral range of width of 1 nm, which approximately corresponds to the width of the spectrum of multifrequency generation in lasers under study, α does not change by more than 0.1° (i.e., much smaller than the error of determination).

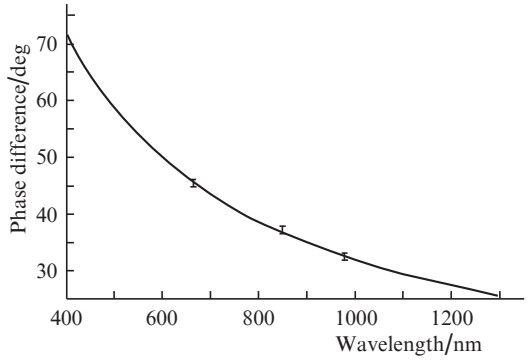

Figure 3. Calibration of the phase plate for the wavelengths λ = 665, 850 and 980 nm and the curve approximating them.

4. Experiment and discussion of the results

To measure the Stokes parameters of radiation of lasers under study, we used the same optical system as that for the calibration of the plate (see Fig. 2) but without the Fresnel rhomb. The polariser was used as an auxiliary tool to set the initial position of optical elements. Before measuring the Stokes parameters, the positions of the polariser and analyser were bound to the X and Y axes in the same way as was done before calibrating the plate. Then, we introduced the plate into the system and oriented its fast axis along the X axis. The criterion for the accurate positioning of the plate was the signal minimum from the photodetector. After that, the polariser was removed from the system and the analyser was rotated by the angle $\pi/2$ such that its initial position corresponded to the X axis (zero for the angle φ).

After setting the initial position of the analyser and the plate we performed quasi-continuous measurement of the intensities $I(\varphi, \psi)$ for four positions of the plate $\psi = 0, \pi/2, \pi$ and $3\pi/2$. Although theoretically $I(\varphi, 0) \equiv I(\varphi, \pi)$ and $I(\varphi, \pi/2) \equiv I(\varphi, 3\pi/2)$, the systematic errors were detected by measuring additionally the data for $\psi = \pi$ and $3\pi/2$. The found dependences were automatically normalised, resulting in the function $I_\psi(\varphi)$. The example of the dependence $I_\psi(\varphi)$ is shown in Fig. 4. The extrema of these functions were used to calculate two values of S_i^{I} and S_i^{II} for each Stokes parameter with the subscript i (i = 1, 2, 3). The parameters of S_i^{I} were determined from expression (9), and the parameters of S_i^{II} were calculated by substituting $a(\psi + \pi)$ and $b(\psi + \pi)$ instead of $a(\psi)$ and $b(\psi)$, respectively, in expression (9). The difference between the obtained values of the parameters S_i^{I} and S_i^{II} can be considered as a quantity characterising the error of their

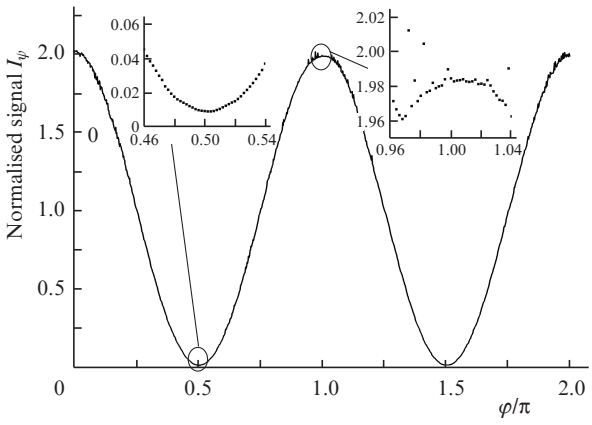

Figure 4. Normalised experimental dependence of the signal from the photodetector on the analyser rotation angle φ. The corresponding Fourier coefficients are $a(\psi) = 0.993$, $b(\psi) = 0.011$. The radiation wavelength is λ = 665 nm.

measurement, which in our case is primarily due to the inhomogeneity of the analyser transmission (systematic component) and fluctuations in the photodetector intensity (statistical component).

To estimate the error, we will analyse the curves $I_\psi(\varphi)$. Thus, according to (9) the error in measuring the Stokes parameters can be taken equal to the error in determining the Fourier components $a(\psi)$ and $b(\psi)$. In turn, $b(\psi)$ in our case can be estimated as the rms value of the Fourier coefficients, corresponding to the period 2π, for a series of curves $I_\psi(\varphi)$. Indeed, the deviation of these coefficients from zero is due either to the inhomogeneity of the analyser transmission or to the noise of the signal from the photodetector, because in the absence of these factors the functions $I_\psi(\varphi)$, according to (6), should have a period of π. This estimate made it possible to establish that the error in measuring the Stokes parameters in our case did not exceed 0.01.

Figure 5 shows the results of all the three Stokes parameters for three lasers at different pump currents. For each value of the current the points show the results of measurements of S_i^{I} and S_i^{II}, which lie within the above empirically defined error ± 0.01. As seen from Fig. 5, the resulting accuracy of the measurements allows one to establish that the second and third Stokes parameters in all the samples under study are nonzero, and also to register their changes as a function of the laser pump current, which suggests the influence of the laser operation regime on the presence and nature of optical inhomogeneities in its cavity. Thus, both the Stokes parameters and their changes might serve as an important quantitative characteristic of the imperfection of the heterostructure layers of which the laser diode is made, as well as an important quantitative characteristic of imperfection of the entire structure of the laser chip. For example, the comparison of data for S_2 and S_3 in Fig. 5 makes it possible to conclude that the optical quality of the cavity of the 665-nm laser diode is about twice better than that of the 850-nm laser diode, but twice worse than the quality of the cavity of the 980-nm laser diode.

Consider now the statistical error. In our case, as mentioned above, this error is caused by the fluctuations in the intensity of laser radiation. These fluctuations were investigated earlier (see, for example, [5] and references therein). To evaluate the fluctuation component in the present study, we performed a series of measurements of the intensity $I(t_j)$, detected by the photodetector for the instants of time t_j at a fixed analyser. Moreover, the number of measurements in one series ($0 \leqslant j \leqslant 1000$) and the time intervals between successive measurements $t_{j+1} - t_j$ were exactly the same as in the measurements of the Stokes parameters for the time T – complete revolution of the analyser.

Then, the obtained sequences of $I(t_j)$ values were considered as different time realisations of the random process. The statistical error was determined as the rms of the Fourier coefficients, normalised by the average intensity, corresponding to the period T and calculated for the dependences $I(t)$. In this case, the error was 0.002. Thus, the statistical error does not exceed systematic error. However, it may become significant if the systematic error is reduced by using higher-quality optical elements.

The question about the possibility of suppressing the statistical error can be answered by determining the spectral dependence of the above mentioned fluctuations directly from the same measurements of $I(t_j)$, which were used to evaluate the statistical error. Figure 6 shows the thus obtained values of the spectral density of fluctuations, which indicate

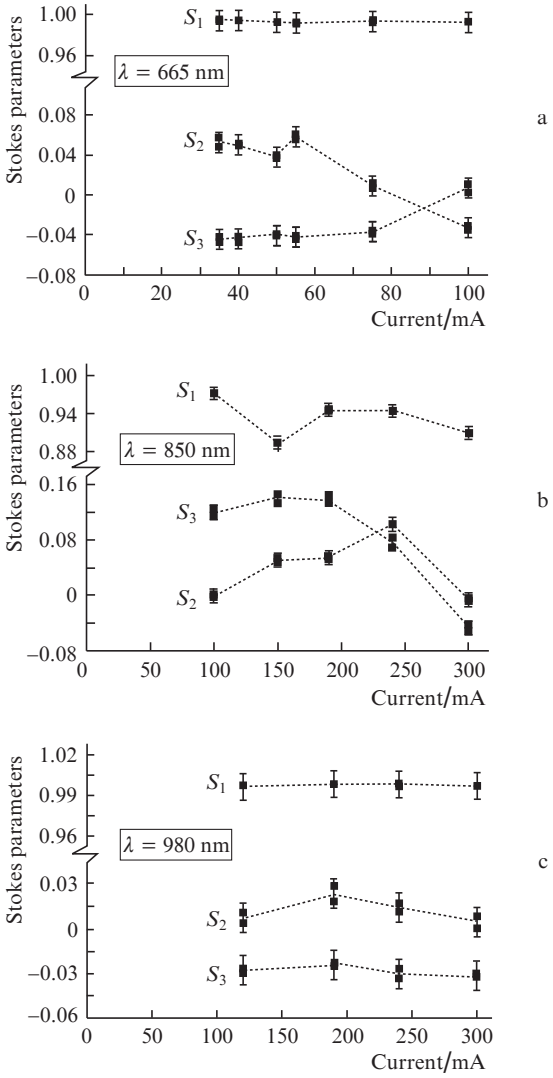

Figure 5. Stokes parameters for laser diodes operating at different wavelengths. For each value of the current we present the values of the S_i^{I} and S_i^{II}, parameters, measured at the phase plate positions differing by the rotation by π. The horizontal lines show the limits of the empirically found error equal to ± 0.01.

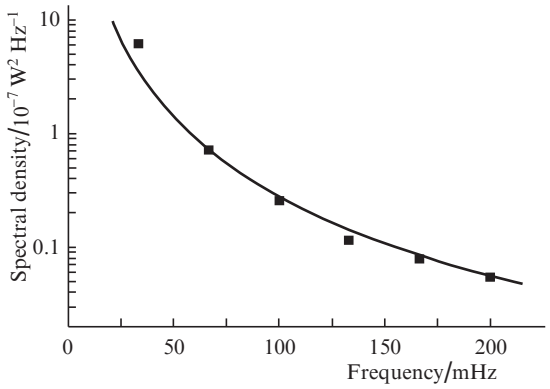

Figure 6. Spectral density of fluctuations of the radiation power measured by the photodetector with a fixed analyser for frequencies greater than and equal to the speed of rotation of the analyser in the basic measurements for a 665-nm laser. Shown in the graph is the approximating curve $G(f) \propto 1/f^{2.3}$.

that the intensity fluctuations are due to the so-called flicker noise with the frequency dependence $G(f) \propto 1/f^{2.3}$. The presence of the flicker noise, characterised by an increase in the growth rate of the spectral density of fluctuations with a decrease in the frequency is a well-known and studied phenomenon, even for diode lasers. The effect of such fluctuations on the measurement accuracy can be lowered, if needed, for example, by increasing the speed of the analyser rotation.

Note in conclusion that although our results show sufficient accuracy of the described techniques for estimating the operation of modern lasers, more advanced laser diodes may require an increase in the accuracy of measurements of the Stokes parameters. In this case, the error of measurements performed with the help of the procedure outlined in the work can be reduced through the use of more advanced optical components. So, instead of film polarisers, it is reasonable to use prism polarisers, and instead of mica plates – high-quality thin quartz ones.

5. Conclusions

The technique presented in this paper allows one, using the same setup, to take measurements of the Stokes parameters of radiation of diode lasers operating in the spectral range from 600 to 1000 nm. Moreover, even the use of ordinary optical elements ensures the measurement accuracy suitable for semiconductor lasers – the accuracy that is sufficient to diagnose the quality of the laser cavities. It is shown that the systematic error in the measurements of the quantities in question is determined by the optical quality of the analyser and the accuracy of the initial position of the optical elements of the system. The statistical error of measurements does not exceed the systematic error and can be effectively suppressed by known methods of elimination of the flicker noise.

References

1. D'yachkov N.V., Bogatov A.P. *Kvantovaya Elektron*., **41** (1), 20 (2011) [*Quantum Electron*., **41** (1), 20 (2011)].
2. Born M., Wolf E. *Principles of Optics* (London: Pergamon, 1970; Moscow: Nauka, 1973).
3. Yariv A., Yeh P. *Optical Waves in Crystals* (New York: Wiley, 1984; Moscow: Mir, 1987).
4. Berry H.G., Gabrielse G., Livingston A.E. *Appl. Opt*., **16** (12), 3200 (1977).
5. Bogatov A.P., Drakin A.E., Plisyuk S.A., Stratonnikov A.A., Kobyakov M.Sh., Zubanov A.V., Marmalyuk A.A., Padalitsa A.A. *Kvantovaya Elektron*., **32** (9), 809 (2002) [*Quantum Electron*., **32** (9), 809 (2002)].